An Enhanced Repetitive Control Algorithm using the Structure of Disturbance Observer

Xu Chen and Masayoshi Tomizuka

Abstract— **In repetitive control, the enhanced servo performance at multiple repetitive frequencies is usually followed by undesired error amplifications at other frequencies. This paper presents a new structural configuration of the internal model principle in repetitive control, wherein designers have more flexibility in the repetitive loop-shaping design, and amplification of non-repetitive errors can be greatly reduced. The proposed algorithm is particularly advantageous when repetitive control is required in environments where large amounts of non-repetitive disturbances exist. Verification of the algorithm is provided in a benchmark regulation problem of hard disk drives.**

I. Introduction

Repetitive control (RC) is a well-known servo design tool for systems that are subjected to periodic disturbances/references. It implements an internal model [1] $1/(1-z^{-N})$ (or $1/(1-e^{-T_p s})$ in the continuous-time case) into a feedback system, such that errors in the previous periods can be used to improve the current regulation/tracking control. Here N and T_p denote respectively the periods of the disturbance/reference in the discrete- and continuous-time cases. Distinguished by its high performance as well as the simple design and implementation criteria, ever since its introduction [2], RC has attracted a great amount of research efforts. Its versatility has been tested in various practical applications, including but not limited to: track-following in magnetic and optical disk drives [3], [4], robot arm control [5], and regulation control in vehicles [6]. For more complete lists of applications, readers can refer to the survey papers [7], [8].

The configuration of the internal model and its interaction with the feedback system vary in literature. The continuous-time RC design mainly applies a series or parallel plug-in configuration [4], [9]–[11]. The prototype discrete-time RC [12], [13] applies the Zero-Phase-Error-Tracking [14] idea and directly cascades a robust version of $1/(1-z^{-N})$ into the open-loop transfer function. Additionally there are plug-in configurations of discrete RC design, among which [15] applies optimization techniques with an extended high-order internal model. Ultimately, a generalized version of $1-z^{-N}$ or $1-e^{-T_p s}$ is absorbed into the denominator of the overall feedback controller, therefore creating high-gain control at the repetitive frequencies (frequencies of the roots of $1-z^{-N}=0$ or $1-e^{-T_p s}=0$). From Bode's Integral Theorem (see, e.g., [16]), enhanced servo performance at certain frequencies commonly results in deteriorated loop shapes at other frequencies. This fundamental limitation, reflected in repetitive control, is the comb-like magnitude response in the sensitivity function, along with undesired gain amplifications at the non-repetitive frequencies (see some examples in [4], [10], [11], [15]).

This paper proposes a new structural RC design with improved loop-shaping properties for digital control. We discuss an approach to extract only the repetitive errors, and introduce the notion of a repetitive disturbance observer (RDOB) as a new RC tool. In the frequency domain, this corresponds to more direct control of the internal model in the closed-loop sensitivity function, leading to greatly reduced gain amplifications at non-repetitive frequencies. An additional benefit of the reduced gain amplification is that the proposed design shows increased ability to reject repetitive errors at high frequencies. A third contribution of the paper is to provide a generalized concept of the disturbance observer (DOB) [17], which has been well-know as a robust control design tool [18]–[21] but, to the authors' best knowledge, has not been discussed in a general context for repetitive control.

II. Controller parametrization

Fig. 1 presents the proposed closed-loop repetitive control scheme. Here $P(z^{-1})$ is the sampled plant (with digital holders) to be controlled. $C(z^{-1})$ is an existing feedback controller designed by any proper loop-shaping methods (e.g., PID or H_∞ control) to achieve the baseline servo performance and robustness. The signals $r(k)$, $y(k)$, $u(k)$, and $d(k)$ are respectively the reference, the plant output, the control input, and the lumped input disturbance.

The proposed RC design is a plug-in compensator that utilizes the internal signals $e(k)$ and $u(k)$ to generate a compensation signal $c(k)$. In the intermediate filtering process in Fig. 1, m denotes the relative degree of $P(z^{-1})$; $P_n^{-1}(z^{-1})$ is a nominal model of $z^{-m}P^{-1}(z^{-1})$; and $Q(z^{-1})$ is a filter to be designed shortly. Notice that $P^{-1}(z^{-1})$ may be anti-causal but we have added delays such that $P_n^{-1}(z^{-1})$ is realizable in Fig. 1. Stability of $P_n^{-1}(z^{-1})$ is required here for internal stability. If the

This work was supported in part by the Computer Mechanics Laboratory (CML) in the Department of Mechanical Engineering, University of California, Berkeley.

The authors are with the Department of Mechanical Engineering, University of California, Berkeley, CA, 94720, USA (email: maxchen@me.berkeley.edu; tomizuka@me.berkeley.edu)

plant model is a minimum-phase system, its inverse can directly be used. Otherwise, the Zero-Phase-Error-Tracking (ZPET) algorithm [14] can be used to obtain a stable $P_n^{-1}(z^{-1})$.

The block diagram applies to regulation and tracking control. In the former case, $r(k)=0$ and the control aim is to reduce $e(k)$ in the presence of the disturbance $d(k)$. In the latter, we aim at maintaining $e(k)$ small w.r.t. a non-zero reference $r(k)$ (i.e., $y(k)$ tracking $r(k)$).

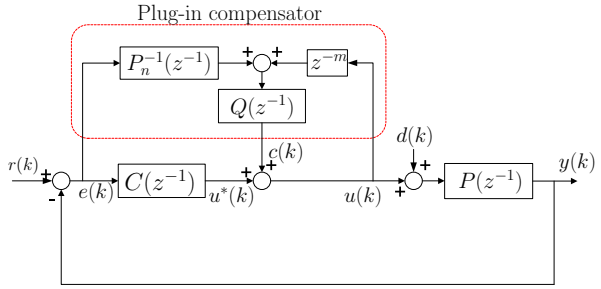

Fig. 1. Block diagram of the proposed repetitive control scheme.

Notice that if $P_n^{-1}(z^{-1})$ is removed from Fig. 1 and $Q(z^{-1})$ is set to $z^{-(N-m)}$, the open-loop transfer function becomes $P(z^{-1})\frac{1}{1-z^{-N}}C(z^{-1})$ and the proposed compensator reduces to a plug-in repetitive controller that is similar to prior arts. To see the intuition of the proposed construction and the new configuration of $Q(z^{-1})$, we first transform the block diagram to the equivalent form in Fig. 2, where we have a unified regulation problem (to keep the fictitious output $-e(k)$ small in the presence of the equivalent disturbances $d(k)$ and $r(k)$). Consider first $r(k)=0$ (the case for rejecting repetitive disturbances). Since $y(k)=P(z^{-1})(u(k)+d(k))$, the output of $P_n^{-1}(z^{-1})$ is given by $P_n^{-1}(z^{-1})P(z^{-1})(d(k)+u(k))$. Notice that $P_n^{-1}(z^{-1})\approx z^{-m}P^{-1}(z^{-1})$. The $P_n^{-1}(z^{-1})$ block thus approximately generates $u(k-m)+d(k-m)$. Subtracting now $u(k-m)$, the output of the z^{-m} block, yields an approximated $d(k-m)$ (i.e., $u_Q(k)=\hat{d}(k-m)$). This forms the idea of a digital disturbance observer (DOB), where $d(k)$ is "observed" by $\hat{d}(k-m)$. Due to the m-step delay, the non-repetitive components in $d(k)$, and the unavoidable modeling errors in $P_n^{-1}(z^{-1})$, $\hat{d}(k-m)$ should not be directly applied to cancel $d(k)$. The idea of the proposed repetitive disturbance observer (RDOB) is to first obtain this estimated $d(k-m)$ and then apply a Q filter that aims at extracting only the repetitive components and counteracting the m-step delay effect. This intuition applies also to the case when $r(k)\neq 0$ (in repetitive reference tracking), where the output of $Q(z^{-1})$ is an approximation of $-P^{-1}(z^{-1})r(k)$.

Fig. 2 differs from conventional DOB-based servo control (see, e.g., [20], [21]) in two aspects. First, the reference $r(k)$ is injected before the $P_n^{-1}(z^{-1})$ block rather than at the summing junction before $C(z^{-1})$. Second, $Q(z^{-1})$ is a customized repetitive signal extractor rather than a low-pass filter. The first point transforms a reference tracking problem to a regulation one, while the second forms a repetitive-control scheme.

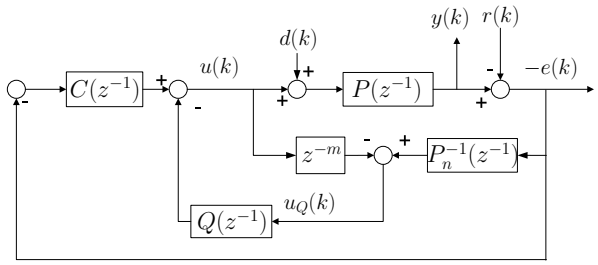

Fig. 2. Equivalent scheme of Fig. 1.

A. Repetitive loop shaping

From Fig. 1, the equivalent controller from $e(k)$ to $u(k)$ is

$$C_{eq}(z^{-1})=\frac{C(z^{-1})+Q(z^{-1})P_n^{-1}(z^{-1})}{1-z^{-m}Q(z^{-1})}, \tag{1}$$

from which we can obtain the sensitivity function (for simplicity, we omit the z-domain index z^{-1} here):

$$S=\frac{1}{1+PC_{eq}}=\frac{1-z^{-m}Q}{1+PC+\left(PP_n^{-1}-z^{-m}\right)Q}. \tag{2}$$

The closed-loop transfer functions from $d(k)$ and $r(k)$ to $e(k)$ are respectively given by

$$G_{ed}(z^{-1})=-P(z^{-1})S(z^{-1}) \tag{3}$$

$$G_{er}(z^{-1})=S(z^{-1}). \tag{4}$$

Assume $r(k)$ and $d(k)$ contain only repetitive components that satisfy

$$\left(1-z^{-N}\right)r(k)=0,\ \left(1-z^{-N}\right)d(k)=0. \tag{5}$$

From (3) and (4), to reject $d(k)$ and $r(k)$, it suffices to have $S(z^{-1})d(k)$ and $S(z^{-1})r(k)$ converge asymptotically to zero. By combining (2) and (5), we can see that this sufficient condition is satisfied if $1-z^{-m}Q(z^{-1})$ contains the term $1-z^{-N}$. To achieve this result, we propose to apply an Infinite Impulse Response (IIR) filter $Q(z^{-1})\triangleq B_Q(z^{-1})/A_Q(z^{-1})$, with the following constraint:

$$A_Q(z^{-1})-z^{-m}B_Q(z^{-1})=1-z^{-N}. \tag{6}$$

Designing $A_Q(z^{-1})=1-\alpha^N z^{-N}$ and solving (6) yield

$$B_Q(z^{-1})=(1-\alpha^N)z^{-(N-m)} \tag{7}$$

$$1-z^{-m}Q(z^{-1})=\frac{1-z^{-N}}{1-\alpha^N z^{-N}}. \tag{8}$$

Notice now in (2), that in regions where the frequency response $P(e^{-j\omega})$ is well modeled by $e^{-jm\omega}P_n(e^{-j\omega})$, the spectral contribution of $\left[P(z^{-1})P_n^{-1}(z^{-1})-z^{-m}\right]Q(z^{-1})$ is small. In the frequency regions where large model mismatch exists, we can make $Q(e^{-j\omega})$ small (in Section II-B) such that the denominator of (2) is still close

to $1+P(z^{-1})C(z^{-1})$. By the above constructions, $S(z^{-1}) \approx \left(1-z^{-m}Q(z^{-1})\right)/\left(1+P(z^{-1})C(z^{-1})\right)$ and the effect of RDOB is directly reflected by $1-z^{-m}Q(z^{-1})$ in the sensitivity function.

In (8), $\alpha(\in[0,1])$ is the ratio between magnitudes of the poles and the zeros in $1-z^{-m}Q(z^{-1})$, and acts as a tuning parameter during loop-shaping. If $\alpha=0$, $Q(z^{-1})$ becomes a Finite Impulse Response (FIR) filter $Q(z^{-1})=z^{-(N-m)}$, which, as discussed before, corresponds to previous RC design. On the other hand, $\alpha=1$ cuts off the repetitive compensation. When $\alpha\in(0,1)$, we have larger flexibility in loop-shaping design. For instance, let $N=10$, $m=1$, and assume a sampling frequency of 26400 Hz. Increasing α from 0 to 0.99 yields the magnitude responses in Fig. 3. We observe that, as α increases towards 1, $1-z^{-m}Q(z^{-1})$ in the top plot has a sharper comb-like magnitude response, and a smaller H_∞ norm (maximum of the magnitude response for single-input-single-output transfer functions). Correspondingly in the bottom plot, $Q(z^{-1})$ behaves as a sharper spectral-selection filter to preserve only the repetitive components in Fig. 2. Specifically, if $\alpha=0$ (the case corresponding to conventional RC), $Q(z^{-1})$ has a magnitude response valued always at 1, losing the spectral-selection property; in the mean time, the maximum value of $1-z^{-m}Q(z^{-1})$ equals $\left\|1-z^{-m}z^{-(N-m)}\right\|_\infty=2$, i.e., disturbances at the corresponding frequencies get amplified by 100% (performance limit of previous RC schemes).

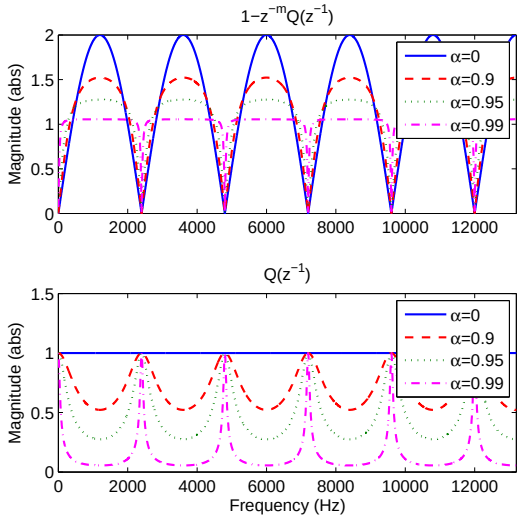

Fig. 3. Magnitude responses of $1-z^{-m}Q(z^{-1})$ and $Q(z^{-1})$.

B. Robust implementation of $Q(z^{-1})$

One central assumption in the previous subsection is the small gain of $\left[P(z^{-1})P_n^{-1}(z^{-1})-z^{-m}\right]Q(z^{-1})$ in (2). It is practically not possible to have an accurate model of $P(z^{-1})$ in the high-frequency region, and thus necessary to incorporate a low-pass filter in $Q(z^{-1})$. It is additionally possible (and recommended) to apply a zero-phase low-pass filter. One simple and flexible way to do this is to construct $q(z,z^{-1})=\prod_j q_j(z,z^{-1})$, where

$$q_i(z,z^{-1})=q_i(z^{-1})q_i(z), \tag{9}$$

$$q_i(z^{-1})=\frac{1-2\cos(\omega_i T_s)z^{-1}+z^{-2}}{2-2\cos(\omega_i T_s)}. \tag{10}$$

Here i is the index number; $\omega_i T_s\in(0,\pi]$. The filter $q_i(z,z^{-1})$ places four zeros to filter out the input spectra at $e^{\pm\omega_i T_s}$, and is normalized by $(2-2\cos(\omega_i T_s))^2$ to have a unity DC gain. The zero-phase property is preserved since the frequency responses of $q_i(z^{-1})$ and $q_i(z)$ are complex conjugates of each other. To have a low-pass structure, we enforce $q(z,z^{-1})$ to contain $q_0(z,z^{-1})=(1+z^{-1})(1+z)/4$ (two zeros at the Nyquist frequency).

We can now construct the practical version of $Q(z^{-1})$ (in comparison with the ideal form from (8)):

$$Q(z^{-1})=\frac{(1-\alpha^N)z^{-(N-m-n_q)}}{1-\alpha^N z^{-N}}z^{-n_q}q(z,z^{-1}), \tag{11}$$

where n_q is the highest order of z in $q(z,z^{-1})$ (so that $z^{-n_q}q(z,z^{-1})$ is realizable). Fig. 4 presents one realization of (11). It is realizable as long as $N-m-n_q\geq 0$. The bandwidth of $q(z,z^{-1})$ can roughly be tuned by comparing the magnitude responses of $\left[P(z^{-1})P_n^{-1}(z^{-1})-z^{-m}\right]Q(z^{-1})$ and $1+P(z^{-1})C(z^{-1})$. A more strict constraint from the stability criteria will be provided in Section III.

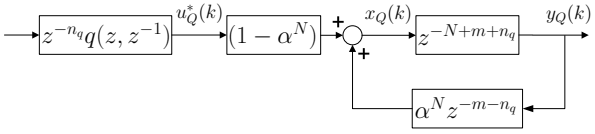

Fig. 4. Implementation of the Q filter.

III. Stability and robust stability

From the previous discussions, if $P_n^{-1}(z^{-1})$ and $Q(z^{-1})$ are properly designed, $\frac{1-z^{-m}Q}{1+PC}$ approximates the sensitivity function in (2), and the closed-loop stability is preserved. Strict nominal closed-loop stability is obtained by using (1) and computing the roots of the characteristics equation from $1+P(z^{-1})C_{eq}(z^{-1})=0$.

When the plant is perturbed to be $\tilde{P}(z^{-1})=P(z^{-1})\left(1+\Delta(z^{-1})\right)$, with a bounded uncertainty $\Delta(z^{-1})$, applying Small Gain Theorem (see, e.g., [16]) yields the following robust stability condition:

$$\left\|\Delta(z^{-1})T(z^{-1})\right\|_\infty<1,$$

where $T(z^{-1})$ is the complementary sensitivity function:

$$T=\frac{PC_{eq}}{1+PC_{eq}}=\frac{CP+P_n^{-1}PQ}{1+CP+Q\left(P_n^{-1}P-z^{-m}\right)}.$$

IV. Transient response

With the plug-in compensator, a new feedback system is formed. In practice, the plug-in module may be activated or deactived depending on actual disturbances. In this high-level control, although the two closed loops are individually well designed, switching between the two stabilizing controllers in general does not yield smooth response [22]. To be more specific, Fig. 4 has the following state-space realization

$$x_Q(k) = (1-\alpha^N)u_Q^*(k) + \alpha^N x_Q(k-N)$$
$$y_Q(k) = x_Q(k-N+m+n_q)$$

where $u_Q^*(k)$, $y_Q(k) \in \mathbb{R}$, and $x_Q(k) \in \mathbb{R}^N$.

Notice that N, the period of the repetitive disturbance/trajectory, can be large. Even if α is close to 1, α^N can be small. When $x_Q(k)$ is initialized to zero, the first $N-m-n_q$ values of $y_Q(k)$ equal zero. Starting from sample $N-m-n_q+1$, $y_Q(N-m-n_q+i) = (1-\alpha^N)u_Q^*(i)$ for $i \in [1,N]$. At this *first* period of actual compensation, depending on the baseline closed-loop dynamics, the impulse of $u_Q^*(k)$ can create high-amplitude transient response in the error signal. Additionally, all the information in $u_Q^*(k)$, including the non-repetitive components, are fed back by the compensation signal, yielding mismatched cancellation for the non-repetitive errors.

In this paper, we apply a time-varying α for transient improvement. It is proposed to initialize α at 1, and exponentially reduce it to the desired final value, following the decay rule

$$\alpha(k+1) = \alpha_{end} - (\alpha_{end} - \alpha(k))\,\alpha_{rate}, \tag{12}$$

with $\alpha(0) = 1$ and the decay rate $\alpha_{rate} \in (0,1)$. Notice that when $\alpha = 1$, the Q filter is essentially turned off ($Q(z^{-1}) = 0$ in (11)). In this way, at the first period of compensation, u_Q^* is gradually (weighted by $1-\alpha^N$) released to y_Q.

As for the settling time of the Q filter, let n_t denote the least number of periods for the impulse response of $Q(z^{-1})$ to reduce to less than 36.8 percent ($\approx e^{-1}$) of its peak value. From (11), we need $(\alpha^N)^{n_t} \le e^{-1}$, yielding

$$n_t = \left\lceil \frac{-1}{\log \alpha^N} \right\rceil, \tag{13}$$

where $\lceil \cdot \rceil$ is the ceiling function.

Therefore, the smaller the term α^N, the shorter the settling time. In the extreme case that $\alpha = 0$, $Q(z^{-1})$ becomes an FIR filter in (11) with $n_t = 1$.

V. Case study

This section provides a design example in the tracking-following control of a hard disk drive (HDD) system. In this study, the disk spins at 7200 revolutions per minute (rpm), and the regulation control aims at positioning the read/write heads to follow the data tracks as precisely as possible. We implement the proposed algorithm to the benchmark problem [23], where the plant is a 14-order system consisting of the dynamics of the power amplifier, the voice-coil motor, and the actuator mechanics. The input and the output of the plant correspond respectively to the (weighted) force input and the position of the read/write heads. At every revolution of the disks, 220 measurements are obtained, at the sampling frequency of 26400 Hz. The period of the repeatable disturbance (synchronized with the rotating disks) is thus $N = 220$, at a base frequency of $7200/60 = 120$ Hz. The baseline controller is an PID controller with several notch filters. The open-loop gain-crossover frequency is 1.19 kHz.

In the RDOB design, we modeled $P(z^{-1})$ to contain the plant as well as the notch filters. Fig. 5 shows the frequency responses of $P(z^{-1})$ and $z^{-m}P_n(z^{-1})$ ($m = 2$ in this example). Since modeling errors appear after around 2 kHz, the zero-phase low-pass filter in Section II-B was designed to have a cut-off frequency of 2025 Hz. In view of the large value of N, α was designed to be 0.999 to achieve good steady-state performance. Correspondingly, α^N became 0.8024. α^N was directly implemented instead of α.

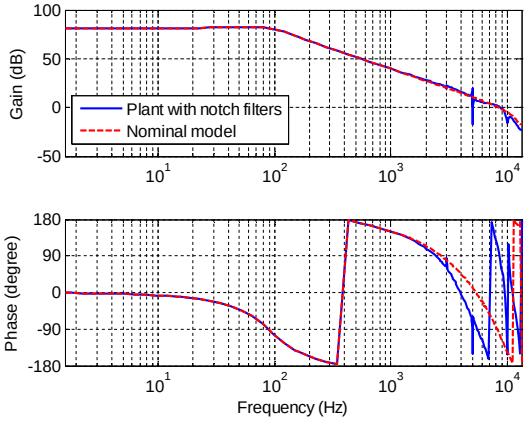

Fig. 5. Frequency responses of $P(z^{-1})$ and $z^{-m}P_n(z^{-1})$.

The magnitude responses of $Q(z^{-1})$ and $1-z^{-m}Q(z^{-1})$ are plotted respectively in the bottom and the top subplots of Fig. 6. Notice the repetitive spectral-selection property (at multiples of the repetitive frequency 120 Hz) in $Q(z^{-1})$, and the gradual reduction of compensation capacity at high frequencies in $1-z^{-m}Q(z^{-1})$. From Fig. 7, we see that the designed loop shape in $1-z^{-m}Q(z^{-1})$ was successfully transformed to the closed-loop system, and that the loop shape at the non-repetitive frequencies was well preserved.

Fig. 8 presents the spectra of the position error signals (PES) (in the steady state) with and without RDOB. One can remark that the repetitive errors below 2000 Hz have been successfully removed, and that amplification of other errors are quite small to be visually distinguished (the multiple spectral peaks between 800 Hz and 1300 Hz were due to the non-repetitive dis-

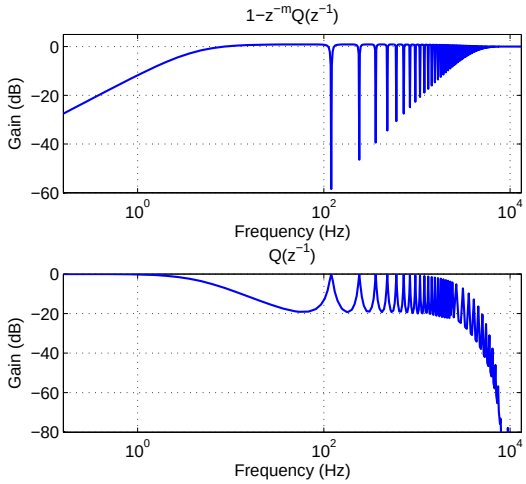

Fig. 6. Magnitude responses of $1-z^{-m}Q(z^{-1})$ and $Q(z^{-1})$.

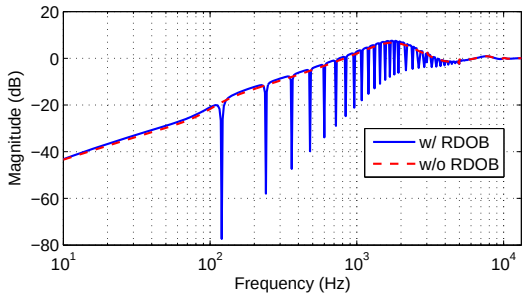

Fig. 7. Magnitude responses of the sensitivity functions.

turbances). As a performance metric in HDD industry, the 3σ (σ denotes the standard deviation) value of the PES reduced from 10.77% Track Pitch (TP) to 9.30% TP, indicating a 13.6 percent improvement.

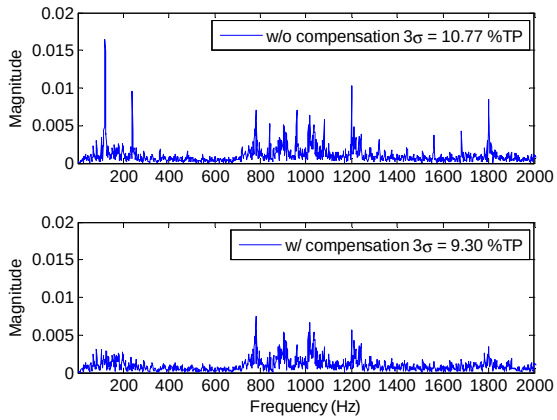

Fig. 8. Spectra of the position errors with and without compensation.

The bottom plot of Fig. 9 shows the PES spectrum using RDOB with $\alpha = 0$, which corresponds to previous RC schemes. It is observed that the repetitive disturbance components were also significantly reduced.

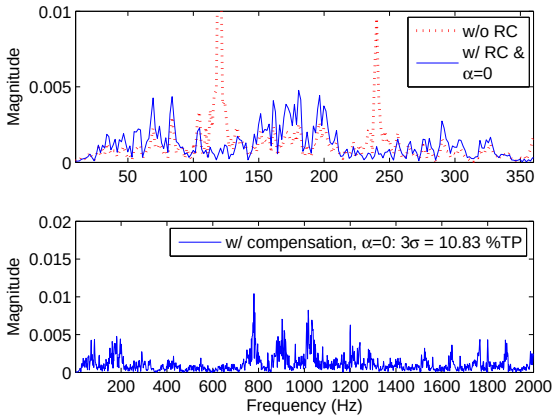

Fig. 9. PES spectrum in RDOB with an FIR Q.

However, due to the amplification of the non-periodic components (see the amplified peaks compared to Fig. 8, and also the enlarged view in the top plot of Fig. 9), the overall 3σ value did not improve but was instead amplified, as can be predicted from the steady-state loop-shaping analysis in Fig. 3. In addition, to avoid excessive high-frequency disturbance amplification, the bandwidth of the zero-phase low-pass filter in $Q(z^{-1})$ was forced to be reduced to 1585 Hz. In this environment that consists of not only repetitive but also a significant amount of non-repetitive disturbances, a conventional RC experienced difficulty improving the overall regulation performance.

To demonstrate further the transient performance, we provide next the simulation results using an additional disturbance profile that is richer in repetitive components. Fig. 10 demonstrates the time traces of the position error signals using different α's in $Q(z^{-1})$. In all cases, the baseline feedback loop had been running for 3 revolutions before RDOB was turned on. On the first subplot, α was maintained at 0.999 throughout the simulation. In the middle and bottom subplots, α was configured to decay from 1 to respectively 0.999 and 0.99. Comparing the top and the middle subplots, we observe that the dynamic switching algorithm provided a much smoother transient response with no visually distinguishable overshoots. Comparing the middle and the bottom subplots in Fig. 9, we see that a smaller α yielded shorter transient response, as predicted by the analysis in Section IV. Note, however, that $\alpha = 0.99$ yielded worse disturbance rejection results at the steady state. This is supported by the analysis in Section II-A. One way to balance the performance is to let α first reduce from 1 to 0.99, and then increase to the final 0.999.

The proposed algorithm has also been successfully implemented to a prototype of industrial wafer-stage system described in [24]. Fig. 11 shows the experiment results during a repetitive scanning process. It is seen

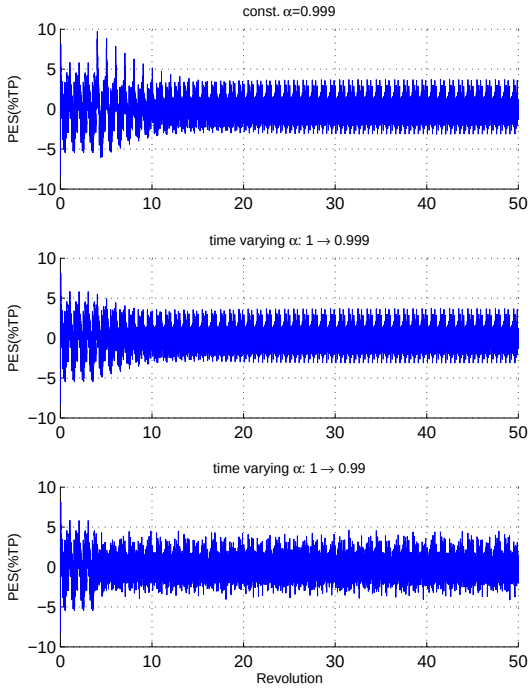

Fig. 10. Transient responses w/ different α's in $Q(z^{-1})$.

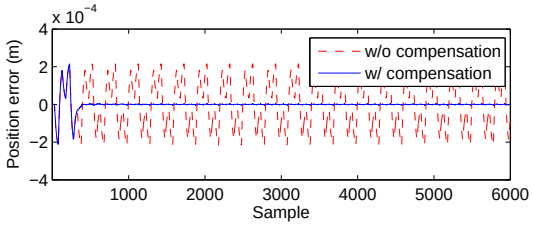

Fig. 11. Experimental verification of RDOB on a wafer stage.

that the proposed algorithm has significantly reduced the tracking errors after just one scanning period.

VI. Conclusion

In this paper, we have discussed a new repetitive control scheme using the structure of Disturbance Observer. From the disturbance-observer perspective, the conventional configuration is extended to address a general class of disturbance spectrum. From the repetitive-control perspective, a new implementation of the internal model principle is proposed, with a corresponding loop-shaping design criteria that enables improved loop shapes. This has an important advantage that repetitive control remains effective in situations where the disturbance has strong non-repetitive frequency components as well as repetitive components.

References

[1] B. A. Francis and W. M. Wonham, "The internal model principle for linear multivariable regulators," *Applied Mathematics & Optimization*, vol. 2, no. 2, pp. 170–194, Jun. 1975.

[2] T. K. S. M. T. Inoue, M. Nakano and H. Baba, "High accuracy control of a proton synchrotron magnet power supply," in *Proc. IFAC World Congress*, 1981, pp. 3137–3142.

[3] K. Chew and M. Tomizuka, "Digital control of repetitive errors in disk drive systems," *IEEE Control Syst. Mag.*, vol. 10, no. 1, pp. 16–20, 1990.

[4] J. Moon, M. Lee, and M. Chung, "Repetitive control for the track-following servo system of an optical disk drive," *IEEE Trans. Control Syst. Technol.*, vol. 6, no. 5, pp. 663–670, 2002.

[5] C. Cosner, G. Anwar, and M. Tomizuka, "Plug in repetitive control for industrial robotic manipulators," in *Proc. 1990 IEEE International Conf. on Robotics and Automation,*, May 1990, pp. 1970 –1975 vol.3.

[6] R. W. Longman, "Iterative learning control and repetitive control for engineering practice," *International Journal of Control*, vol. 73, no. 10, pp. 930–954, 2000.

[7] G. Hillerström and K. Walgama, "Repetitive control theory and applications-a survey," in *Proc. 13th IFAC World Congress*, 1996, pp. 1–6.

[8] C. Li, D. Zhang, and X. Zhuang, "A survey of repetitive control," in *Proc. 2004 IEEE/RSJ International Conf. on Intelligent Robots and Systems*, vol. 16, no. 7, Jan. 2004, pp. 1160 – 1166.

[9] S. Hara, Y. Yamamoto, T. Omata, and M. Nakano, "Repetitive control system: a new type servo system for periodic exogenous signals," *IEEE Trans. Autom. Control*, vol. 33, no. 7, pp. 659 –668, Jul 1988.

[10] K. Srinivasan and F.-R. Shaw, "Analysis and design of repetitive control systems using the regeneration spectrum," in *Proc. American Control Conf.*, May 1990, pp. 1150 –1155.

[11] M.-C. Tsai and W.-S. Yao, "Design of a plug-in type repetitive controller for periodic inputs," *IEEE Trans. Control Syst. Technol.*, vol. 10, no. 4, pp. 547 –555, jul 2002.

[12] M. Tomizuka, T.-C. Tsao, and K.-K. Chew, "Analysis and synthesis of discrete-time repetitive controllers," *ASME Journal of Dynamic Systems, Measurement, and Control*, vol. 111, no. 3, pp. 353–358, 1989.

[13] M. Tomizuka, "Dealing with periodic disturbances in controls of mechanical systems," *Annual Reviews in Control*, vol. 32, no. 2, pp. 193 – 199, 2008.

[14] ——, "Zero phase error tracking algorithm for digital control," *ASME Journal of Dynamic Systems, Measurements, and Control*, vol. 109, no. 1, pp. 65–68, 1987.

[15] G. Pipeleers, B. Demeulenaere, J. De Schutter, and J. Swevers, "Robust high-order repetitive control: optimal performance trade-offs," *Automatica*, vol. 44, no. 10, pp. 2628–2634, 2008.

[16] J. C. Doyle, B. A. Francis, and A. Tannenbaum, *Feedback control theory*. Macmillan, 1992, vol. 134.

[17] K. Ohnishi, "Robust motion control by disturbance observer," *Journal of the Robotics Society of Japan*, vol. 11, no. 4, pp. 486–493, 1993.

[18] C. J. Kempf and S. Kobayashi, "Disturbance observer and feedforward design for a high-speed direct-drive positioning table," *IEEE Trans. Control Syst. Technol.*, vol. 7, no. 5, pp. 513–526, 1999.

[19] M. White, M. Tomizuka, and C. Smith, "Improved track following in magnetic disk drives using a disturbance observer," *IEEE/ASME Trans. Mechatronics*, vol. 5, no. 1, pp. 3–11, Mar. 2000.

[20] K. S. Eom, I. H. Suh, and W. K. Chung, "Disturbance observer based path tracking control of robot manipulator considering torque saturation," *Mechatronics*, vol. 11, no. 3, pp. 325 – 343, 2001.

[21] K. K. Tan, T. H. Lee, H. F. Dou, S. J. Chin, and S. Zhao, "Precision motion control with disturbance observer for pulsewidth-modulated-driven permanent-magnet linear motors," *IEEE Trans. Magn.*, vol. 39, no. 3, pp. 1813–1818, 2003.

[22] D. Liberzon and A. Morse, "Basic problems in stability and design of switched systems," *IEEE Control Syst. Mag.*, vol. 19, no. 5, pp. 59–70, 1999.

[23] IEEJ, Technical Commitee for Novel Nanoscale Servo Control, "NSS benchmark problem of hard disk drive systems," http://mizugaki.iis.u-tokyo.ac.jp/nss/, 2007.

[24] S. Mishra, W. Yeh, and M. Tomizuka, "Iterative learning control design for synchronization of wafer and reticle stages," *2008 American Control Conf.*, pp. 3908–3913, Jun. 2008.